



Deposited via The University of Sheffield.

White Rose Research Online URL for this paper:

<https://eprints.whiterose.ac.uk/id/eprint/213346/>

Version: Published Version

Article:

Jiang, J., Cui, H., Bhople, P. et al. (2024) Biochar combined with garbage enzyme enhances nitrogen conservation during sewage sludge composting: evidence from microbial community and enzyme activities related to ammoniation. *Agronomy*, 14 (6). 1162. ISSN: 2073-4395

<https://doi.org/10.3390/agronomy14061162>

Reuse

This article is distributed under the terms of the Creative Commons Attribution (CC BY) licence. This licence allows you to distribute, remix, tweak, and build upon the work, even commercially, as long as you credit the authors for the original work. More information and the full terms of the licence here:

<https://creativecommons.org/licenses/>

Takedown

If you consider content in White Rose Research Online to be in breach of UK law, please notify us by emailing eprints@whiterose.ac.uk including the URL of the record and the reason for the withdrawal request.

Article

Biochar Combined with Garbage Enzyme Enhances Nitrogen Conservation during Sewage Sludge Composting: Evidence from Microbial Community and Enzyme Activities Related to Ammoniation

Jishao Jiang ^{1,*}, Huilin Cui ¹, Parag Bhole ², Caspar C. C. Chater ^{3,4} , Fuqiang Yu ⁵  and Dong Liu ^{5,*} 

- ¹ Henan Key Laboratory for Environmental Pollution Control, Key Laboratory for Yellow River and Huai River Water Environmental Pollution Control, Ministry of Education, School of Environment, Henan Normal University, Xinxiang 453007, China; 2219183018@stu.htu.edu.cn
- ² Crops, Environment, and Land Use Department, Environment Research Centre, Teagasc, Johnstown Castle, Y35 TC98 Wexford, Ireland; paraghoplebt@gmail.com
- ³ Royal Botanic Gardens, Kew, Richmond TW9 3AE, UK; caspar.chater@gmail.com
- ⁴ Plants, Photosynthesis, and Soil, School of Biosciences, University of Sheffield, Sheffield S10 2TN, UK
- ⁵ The Germplasm Bank of Wild Species, Yunnan Key Laboratory for Fungal Diversity and Green Development, Kunming Institute of Botany, Chinese Academy of Sciences, Kunming 650201, China; fqyu@mail.kib.ac.cn
- * Correspondence: jiangjishao@htu.edu.cn (J.J.); liudongc@mail.kib.ac.cn (D.L.)

Abstract: Nitrogen loss is an unavoidable problem during composting processes, and the ammonia oxidation process significantly affects nitrogen transformation. The objective of this study was to evaluate nitrogen transformation when garbage enzyme (GE), biochar (BC), pelolith (PL) and combinations thereof were added during sewage sludge composting. Meanwhile, the succession of ammonia-oxidizing bacteria (AOB) and archaea (AOA) were also explored via quantitative polymerase chain reaction and high-throughput sequencing. The results showed that GE + BC and GE + PL treatments decreased ammonia (NH₃) formation by 23.8% and 8.3%, and that of nitrous oxide (N₂O) by 25.7% and 26.3% relative to the control, respectively. Simultaneously, the GE, GE + BC, and GE + PL treatments boosted the succession of AOA and AOB, and increased the activities of ammonia monooxygenase (AMO) and hydroxylamine oxidoreductase (HAO) activities and the gene copies of AOA and AOB. The AMO activities, NH₄-N, NO₃-N, and C/N, significantly affect AOA and AOB community structures. The network analysis predicted that the AMO and HAO were secreted mainly by the *unclassified_Archaea* and *norank_Crenarchaeota*, whereas it also showed that the GE + BC improved microbial associations with AOA, enzymatic activity, and environmental factors. Thus, the addition of garbage enzyme and biochar appears to be a promising mitigation strategy to reduce nitrogen losses during the composting process.

Keywords: composting; sewage sludge; biochar; ammonia oxidase; ammoniation



Citation: Jiang, J.; Cui, H.; Bhole, P.; Chater, C.C.C.; Yu, F.; Liu, D. Biochar Combined with Garbage Enzyme Enhances Nitrogen Conservation during Sewage Sludge Composting: Evidence from Microbial Community and Enzyme Activities Related to Ammoniation. *Agronomy* **2024**, *14*, 1162. <https://doi.org/10.3390/agronomy14061162>

Academic Editors: Halyna Kominko and Grzegorz Izydorczyk

Received: 10 May 2024

Revised: 25 May 2024

Accepted: 28 May 2024

Published: 29 May 2024



Copyright: © 2024 by the authors. Licensee MDPI, Basel, Switzerland. This article is an open access article distributed under the terms and conditions of the Creative Commons Attribution (CC BY) license (<https://creativecommons.org/licenses/by/4.0/>).

1. Introduction

Composting is an effective method of harmless utilization and recycling of organic solid waste into high-quality environmentally friendly organic fertilizers [1]. As a kind of fertilizer, nitrogen (N) content has been the main standard to evaluate the quality of compost, thus N cycling is of central importance among other aspects such as humification and greenhouse gases [2–4]. During composting, the N loss, in the form of ammonia (NH₃) via the transformation of ammonium-N (NH₄-N) through ammonification, was generated during the composting process [5]. However, NH₄-N could strategically be converted into nitrate (NO₃-N) through nitrification, effectively controlling N loss in the form of NH₃ emissions [6]. This nitrification is directly impacted by ammonia oxidizers through the ammoxidation process, which likely changes the subsequent N cycle and the compost

quality as well [7]. Therefore, it becomes highly important to explore the community succession pattern of microorganisms related to ammonia oxidation and their convulsive effects on composting processes.

Bacteria and archaea both are potential ammonia oxidizing microorganisms (ammonia oxidizing bacteria—AOB, and ammonia-oxidizing archaea—AOA) during the process of composting. However, to date, the consensus about AOA or AOB regarding their predominance during composting is inadequate. Zeng et al. [8] reported that gene copies of AOA were more abundant, while AOB were not detected during the thermophilic and cooling stages of the composting of agricultural waste. Yan et al. [9] also reported that AOA outnumber AOB by 2–3 times during cattle manure composting. Contrastingly, Wu et al. [10] recently reported that AOB played the dominant role in comparison to the AOA during the composting of agricultural waste when zeolite and biochar were used as substrates. Previously, Yan et al. [9] had also found similar results during cattle manure composting. These ambiguities demonstrate that community diversity and the quantity of AOA and AOB may be differentially impacted by various factors, such as the raw materials used for composting and the temperature, moisture content, and O₂ concentration, warranting further investigation. In addition, ammonia monooxygenase (AMO) and hydroxylamine oxidoreductase (HAO) were the main enzymes reported during the ammonia oxidation process [11], which directly determined the final NO₃-N content of the compost. The NH₄-N is first converted into hydroxylamine (NH₂OH) using AMO, and then this product may further be oxidated to nitrite by HAO [12]. However, to date, the quantification and reactivity levels of AMO and HAO during organic solid-waste composting has been limited.

The N from the compost can be reserved and the quality of the end compost product could be enhanced by adding appropriate additives. A fermentation solution of waste vegetables and fruits, along with water and brown sugar, called garbage enzyme (GE), has been widely used in wastewater treatment, soil fertilizer, and heavy metal ion absorption research [13], mainly because of its functional capacities to decompose, compose, transform, and catalyze any chemical reaction [13]. However, due to its low pH (~3.3 units) GE could potentially slow down the growth of microorganisms and prolong the composting process [14]. In addition, it is well known that biochar (BC) and peletith (PL) are widely used additives during organic waste composting that reduce NH₃ emissions and N loss. Their usage is mainly based on their high total-pore volume and adsorption capacities [15], which increase porosity and eliminate anaerobic pocket formation [16,17]. Used together, BC and PL could provide habitat and refuge for bacteria, protect bacteria from low pH levels, and the generate high temperatures via high specific surface area and total pore volume [18]. Furthermore, BC contains alkali metal salts and organic functional groups, and thus has a strong pH-buffering capacity [19]. These advantages are likely to regulate the succession of ammonia oxidizers and improve the ammonia oxidation process, ultimately reducing N loss. Furthermore, BC and PL are inexpensive and convenient, which makes them ideal additives for organic waste composting. However, only a few studies have attempted to evaluate the effects on composting processes and the successions of AOA and AOB of GE combined with BC or PL.

Therefore, the objectives of this research were: (i) to gain insights into the effects of BC and PL combined with GE on N transformation and the activities of AMO and HAO enzymes; (ii) to quantify gene copies and identify the community composition and succession patterns of the AOA and AOB during organic composting; and, finally, (iii) to find the environmental factors driving changes in AOA and AOB community dynamics during the composting of sewage sludge.

2. Materials and Methods

2.1. Raw Materials, Additives, and Design

A laboratory simulation of the composting experiment was conducted at the School of Environment, Henan Normal University (Xinxiang, China; N 35°19′39.522″, E 113°54′55.613″)

for 24 days. The raw materials were dewatered sewage sludge (SS) and saw dust (SD), which were obtained from the Xiaoshangzhuang sewage treatment plant and a local furniture factory in Xinxiang, respectively. The physicochemical characteristics of the sewage sludge have been reported in our previous work [20,21]. The GE was prepared according to the procedure described by Arun and Sivashanmugam [13] using a mixture of brown sugar, waste fruits, and water. The characteristics of the GE were: pH, 3.1; total organic carbon (TOC), 3.1 g L⁻¹; and total nitrogen (TN), 4.1 g L⁻¹, respectively. The BC was purchased from the pingdingshan green source activated carbon Co., Ltd., where the primary material used was wood pellets. Meanwhile, the BC and PL were shredded to a size of 3–5 mm particles, with the total pore volume (TPV) of 0.05 and 0.02 cm³ g⁻¹, and a BET surface area (SSA) of 14.2 m² g⁻¹ and 6.5 m² g⁻¹, respectively.

The composting experiments consisted of four different treatments. Fresh SS and SD were mixed in a ratio of 4:1 and used as the control treatment. The second treatment, marked as GE, received 2% GE solution (on a dry weight basis). The third treatment (BC + GE), received a 2% GE solution and 10% BC (on a dry weight basis). Finally, the fourth treatment (BC + PL) was composed of a 2% GE solution and 10% PL. The fermentation process refers to a similar procedure to the one described by Jiang et al. [20,21]. During the composting process, sufficient O₂ was supplied by periodical turning and ventilating of the composting pile: 4 instances of ventilating and 2 of turning, during the first 12 days; with only 2 instances of ventilating during the final 13–24 days.

2.2. Sampling and Determination of Physicochemical Properties

The compost was sampled on days 0, 4, 8, 13, and 24 according to temperature changes. Before sampling, the composting mixture needed to be overturned evenly. Three samples from each treatment were collected and stored separately. Each sample was further divided into four parts of which one part was used for the analysis of the total nitrogen (TN) after air-drying. The second part was used to measure physicochemical indexes and enzymatic activities, and was stored at a cool temperature of 4 °C until analysis. While the fourth part was immediately frozen at –80 °C for microbial assays. The NH₃ and N₂O emissions were measured through a portable gas detector [22,23]. A compost extract was obtained from the mixture of compost and deionized water with a ratio of 1:10 (*w/v*). After centrifugation and filtration, the pH, EC, NO₃-N, and NH₄-N were measured by following standard laboratory methods [24]. The TN concentration of the pulverized samples was analyzed by an elemental analyzer (Elemental Vario EL, Frankfurt, Germany) [23].

2.3. Enzyme Activity Analysis

Quantification with fluorescein diacetate as a substrate: Fluorescein diacetate hydrolase (FDA) activity was measured at 620 nm using a colorimetric method. The AMO activity of the composting samples was determined using the AMO ELISA kit, and calculated at 420 nm using a colorimetric method [10]. To measure HAO activity, the samples were subjected to a reaction system, which consisted of compost extract, K₃[Fe(CN)₆] (0.01 mol/L), EDTA (0.04 mmol/L), Tris-HCl (10 mmol/L), and HONH₃Cl-N (15 mg/L). The system was placed in a water bath at 25 °C for 5 min, and the decrease in K₃Fe(CN)₆ per minute was measured to quantify HAO activity [25].

2.4. Microbial Analysis

Composting samples on days 4, 13, and 24 were selected to study the structure and quantity of the AOA and AOB. Total genomic DNA was extracted from a 0.5 g compost sample according to the instructions of the MoBioPowerSoil[®] DNA Isolation Kit (12888) (MO BIO Laboratories, Inc., Carlsbad, CA, USA). The quality of genomic DNA was determined by 1% agarose gel electrophoresis, followed by NanoDrop2000 (Thermo Scientific Company, Waltham, MA, USA) to determine the DNA concentration and purity. The AOB and AOA gene copies were detected by q-PCR using an ABI 7300 fluorescence quantitative PCR instrument (Applied Biosystems, Waltham, MA, USA) with

the primers Arch-amoAF (STAATGGTCTGGCTTAGACG)/Arch-amoAR (GCGGCCATC-CATCTGTATGT) and AmoA-1F (GGGGTTTCTACTGGTGTT)/AmoA-1R (CCCCTCK-GSAAAGCCTTCTTC), respectively [10]. The OD₂₆₀ values of AOA and AOB plasmids were measured with a UV spectrophotometer (NanoDrop2000, Thermo Fisher Scientific, USA) and then converted into a copy number to draw a standard curve. The linearity (R^2) of the standard curves of AOA and AOB genes was 0.9986 and 0.9999, respectively.

Using the previously extracted DNA as a template, PCR amplification of the archaeal and bacterial 16S rRNA gene was performed with the same primers as stated above. The thermal cycling steps for PCR amplification of AOA and AOB were: pre-deformation at 95 °C for 3 min, 1 cycle; deformation at 95 °C for 30 s; annealing at 55 °C for 30 s and extension at 72 °C for 45 s for a total of 27 cycles; and final extension at 72 °C for 10 min (PCR instrument: ABI GeneAmp[®] 9700, Foster City, CA, USA). The 16S rDNA sequences of the AOA and AOB genes were analyzed using the Illumina MiSeq paired-end 300 bp protocol (Illumina, Inc., San Diego, CA, USA).

2.5. Statistical Analyses

All indicator data were collected in triplicate. IBM SPSS Statistics 20.0 was used to calculate the mean \pm standard deviation of the physicochemical indexes and enzymes. The differences in enzymatic activities were evaluated by principal component analysis (PCA) using CANOCO 5.0. While the online platform i-Sanger (<http://www.i-sanger.com/>, accessed on 1 June 2023) was used to conduct AOA and AOB microbial community diversity analyses. Correlations between the environmental factors, enzyme activities, and microbial community composition of AOA and AOB were assessed by redundancy analysis (RDA) using CANOCO 5.0. However, many environmental factors can affect the distribution of the microbial structure during the process of composting, but many of them have a strong collinearity. Therefore, the driving environmental factor should be screened prior to environmental factor analysis in order to remove the factors that have a strong collinearity. In the present study, the variance inflation factor (VIF) was measured and the environmental factors with a VIF > 20 were removed from the subsequent analysis. Based on the results of the VIF values (Table S1), pH, TOC, TN, and HAO were removed. Therefore, only the EC, MC, NH₄-N, NO₃-N, C/N, FDA, and AMO were used for the redundancy analysis (RDA) using Canoco 5.0 software.

3. Results and Discussion

3.1. Dynamic Changes in the NH₃ and N₂O Emissions

NH₃ and N₂O emissions are the main sources of N loss during a well-controlled composting process [26,27]. As shown in Figure 1a, the NH₃ emitted during the days 3–12 made up approximately 82.0–88.2% of the total gas emissions. With rapid decomposition of the organic matter (OM), the NH₃ emissions increased quickly at the initial stage and reached to the maximums on day 6 for all treatments except the GE + BC treatments on day 8. The maximum emissions of NH₃ occurred at levels of 81.4, 43.9, 70.5, and 71.3 mg/d in the CK, GE, GE + BC, and GE + PL treatments, respectively. After the 8th day of the composting process, the NH₃ emissions were stable and similar to those observed on day 1. During the whole process, the cumulative NH₃ emissions in the treatments of the CK, GE, GE + BC, and GE + PL treatments were 528, 307, 402, and 485 mg, respectively (Figure 1a). Compared to CK, the NH₃ emissions in the GE, GE + BC, and GE + PL treatments reduced by 41.8%, 23.8%, and 8.3%, respectively. These results indicate that additives were effective in compensating the loss of N via NH₃ emissions. These results are in line with previous studies, which suggested that the low-pH and enzyme-rich activities of GE and the adsorption capacity of BC and PL are major sources of reduced N mineralization in composting processes where GE and BC or PL were used as a process catalyst and additives, respectively [17]. However, in our study, the values in the GE + BC and GE + PL treatments were significantly higher than the GE treatments. It can be said that the benefits of adding BC and PL may have been underestimated in previous studies

and that such additions are far more advantageous for the growth of microorganisms, strengthening the ammonification process compared to the GE-only treatments with no additives [28]. In addition, the SSA and TPV of BC during different composting processes were all greater than the PL during the entire composting process (Table 1); therefore, the GE + BC treatments may further adsorb additional NH₃ compared to the GE + PL treatments and, ultimately, may result in reduced NH₃ emissions.

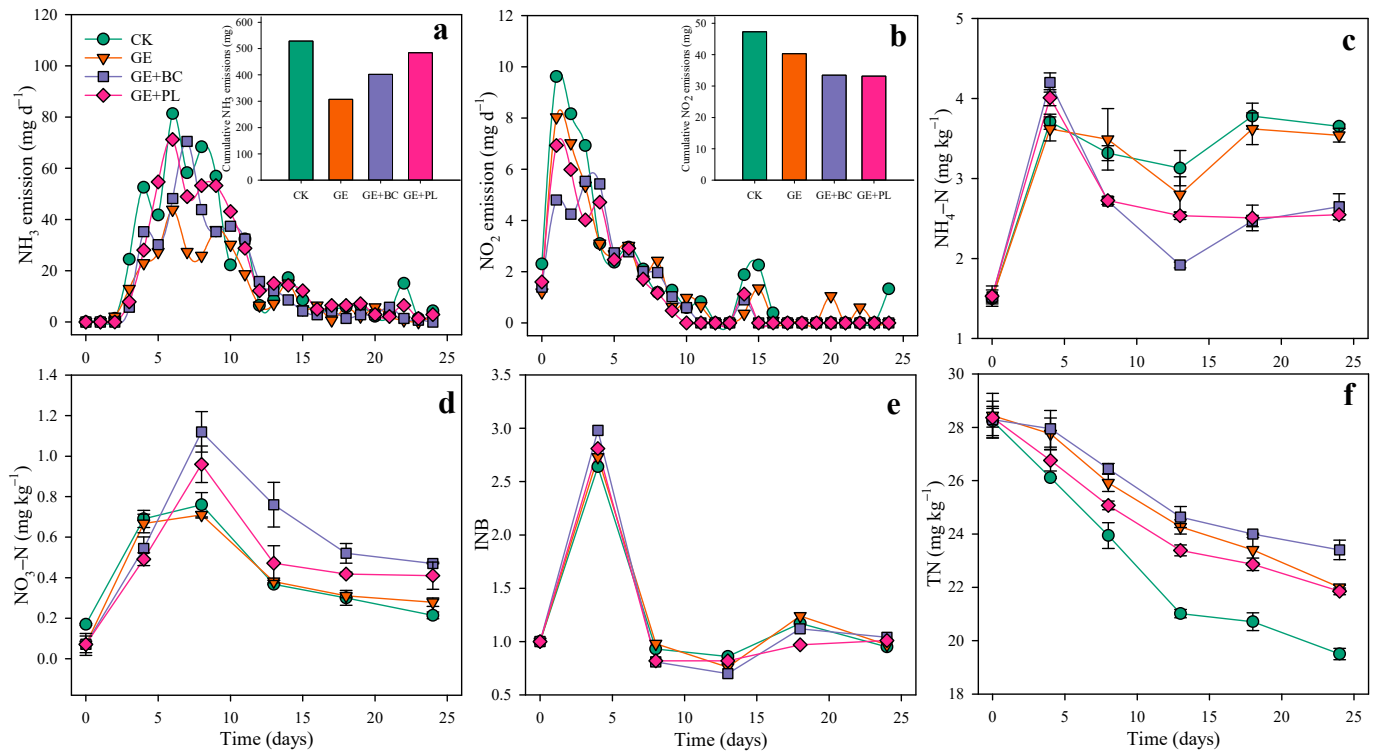


Figure 1. NH₃ (a), N₂O (b) emissions, NH₄-N (c), NO₃-N (d), the INB index (e), and TN (f).

Table 1. Changes in specific surface areas (SSA) and total pore volume (TPV) of PL and BC during the composting process.

Composting Time (Days)	BC		PL	
	SSA (m ² g ⁻¹)	TPV (cm ³ g ⁻¹)	SSA (m ² g ⁻¹)	TPV (cm ³ g ⁻¹)
0	14.19 ± 0.34	0.050 ± 0.001	6.53 ± 0.26	0.019 ± 0.001
4	7.23 ± 0.11	0.039 ± 0.002	3.49 ± 0.11	0.021 ± 0.003
8	6.54 ± 0.38	0.038 ± 0.003	2.35 ± 0.23	0.022 ± 0.002
13	6.13 ± 0.64	0.034 ± 0.001	4.00 ± 0.88	0.023 ± 0.009
18	6.11 ± 0.40	0.035 ± 0.001	2.80 ± 0.30	0.017 ± 0.006
24	5.34 ± 0.35	0.035 ± 0.005	3.16 ± 0.15	0.015 ± 0.001

Similar to the NH₃ emissions, the intensity of N₂O emissions was higher during the initial thermophilic period (days 1–6) (Figure 1b), and similar results were also found that by Awasthi et al. [15] during composting. The peak values of N₂O emissions appeared on day 1 with the values of 9.6, 8.0, and 6.9 mg d⁻¹ in the CK, GE, and GE + PL treatments, respectively, while the GE + BC treatments on day 3 had a value of 5.5 mg d⁻¹. The cumulative N₂O emissions for the four treatments were 47.3, 40.3, 33.5, 33.1 mg, respectively. The three additive treatments showed reduced emissions of N₂O by 10.4%, 25.7, and 26.3% relative to the control treatment. Geng et al. [29] reported that biochar could reduce cumulative N₂O releases by 47.7% during kitchen waste composting. The BC and PL not only have a large SSA that can adsorb the emitted N₂O, but also may increase the TPV of the composting pile and impede the formation of an anaerobic environment, thus

further decreasing the N₂O emissions caused by the denitrification process and mediated by denitrifying microbial communities.

3.2. Dynamic Changes in NH₄-N, NO₃-N, and TN Concentrations

NH₄-N is the substrate directly acted upon by the ammonia-oxidizing microorganisms and, therefore, has a significant influence on subsequent nitrification processes [30]. The NH₄-N content increased sharply (Figure 1c) because of the intense decomposition of nitrogen from the organic substrate where all treatments showed maximum values on day 4, in a range of 3.71, 3.62, 4.20, and 4.01 mg kg⁻¹. The values for GE + BC and GE + PL were greater than those for the CK and GE treatments, which might be attributed to the low pH of GE, which may slightly inhibit the decomposition of organic matter [23]. Meanwhile, the BC and PL alleviated the inhibition of GE, promoted the degradation of organic matter, and effectively absorbed the emitted NH₃ [17]. Following this, the NH₄-N contents in the GE + BC and GE + PL treatments showed an obvious decrease certainly due to the intense nitrification and, therefore, perhaps not greatly different within the CK and GE treatments. At the end of the composting process, the NH₄-N contents for the GE + BC and GE + PL treatments (2.65 and 2.55 mg kg⁻¹) were less than those for CK and GE (3.65 and 3.54 mg kg⁻¹).

Similarly, the NO₃-N contents firstly increased during days 0–8 and then decreased until the end of the composting period (Figure 1d). This is in line with the previous study conducted on SS composting [17]. The difference was that the maximum NO₃-N contents appeared on day 8, which lagged behind the peak values of the NH₄-N contents. Except for days 0 and 4, the NO₃-N contents for the GE + BC and GE + PL treatments were higher than those for the CK and GE treatments. At the end of composting period, the NO₃-N contents for the four treatments were 0.21, 0.28, 0.47, and 0.41 mg/kg, respectively, and in the order of GE + BC > GE + PL > GE treatment (123.8%, 95.2%, 32.9%) relative to the control treatment. Together with those of NH₄-N, the overall results showed the GE + BC and GE + PL treatments enhanced ammonification and nitrification during the composting process, thus improving the NO₃-N content of the end compost.

The index of the N balance (INB) was used to evaluate the total variation in dissolved inorganic N in the incubation system, such as the soil incubation and wastewater treatment, which was calculated based on the previous study [31]. As shown in Figure 1e, the INB in all treatments sharply increased during days 0–4 in all treatments, and then began to decrease gradually during the latter 4–8 days. The values of INB during days 0–4 ranged from 0.81 to 2.98, suggesting that the N loss was a result of the ammonification of the organic N during this stage [31]. The NH₃ emissions via ammonification during days 0–4 could be explained by this phenomenon (Figure 1a). And then, the INB became almost near 1.0, which indicates no remarkable amount of DIN production from organic matter and no N loss emitted from NH₃ and N₂O during this stage [32].

Figure 1f shows the TN content for all four treatments with a descending trend during the whole composting process. The rapid decrease during days 0–12 was likely because of the intense emissions of NH₃ and N₂O (Figure 1a,b). The TN contents of the end compost in the CK, GE, GE + BC, and GE + PL treatments therefore reduced by 30.9%, 22.6%, 23.4%, and 21.9% relative to the initial values. This indicated that the BC and PL were correlated with GE and effectively reduced the N loss from NH₃ and N₂O emissions, especially within the GE + BC treatment.

3.3. Dynamic Changes in FDA, AMO, and HAO Activities

Figure 2a shows that the additives (in the GE, GE + BC, and GE + PL treatments) significantly increased the fluorescein diacetate hydrolase (FDA) activities at the initial stage relative to the control treatment, and the activity of FDA for the GE + BC treatments were always highest among the four treatments during the whole composting process. During the whole stage, the FDA activities of the four treatments declined. Although, these results were inconsistent with our previous study [17], showing maximum FDA activities in

the similar treatment of additives on day 4. However, an intense decrease in FDA activities in this study in the GE, GE + BC, and GE + PL treatments was detected during days 0–4. This can be attributed to the fact that, during this stage, the OM contents decreased rapidly and all the FDA enzymes in the system were consumed, leaving the system enzyme-deficient in the latter stages. This phenomenon needs further investigation and can be a potential objective in forthcoming studies.

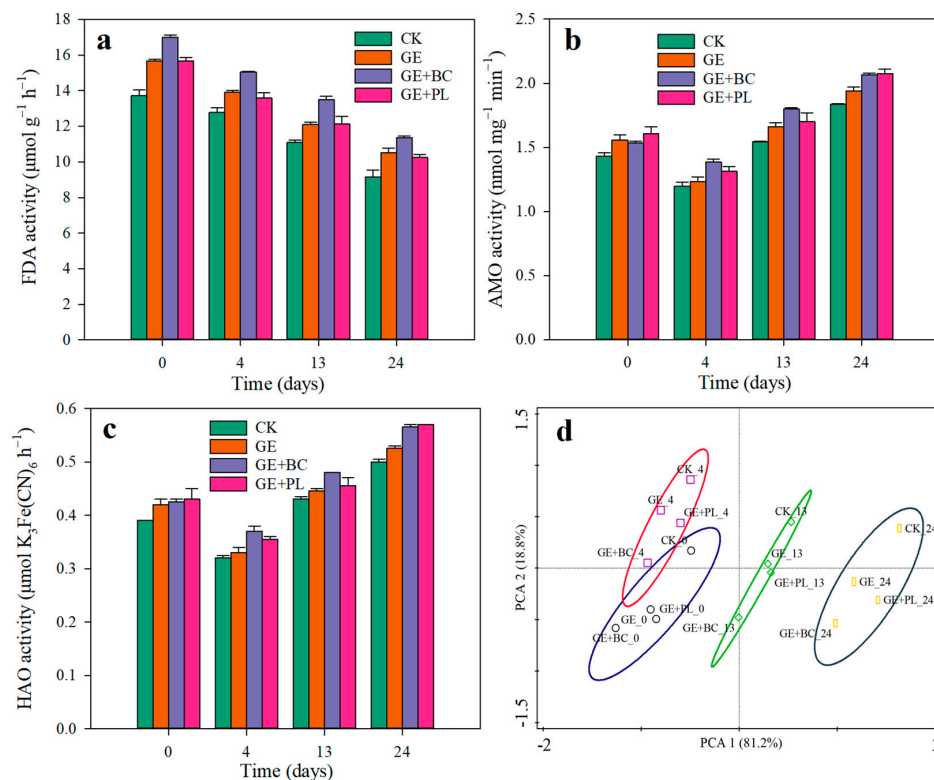


Figure 2. The activities of FDA (a), AMO (b), HAO (c), and the principal component analysis of FDA, AMO, and HAO (d).

Few studies have focused on AMO activities during the composting process, while most studies have always evaluated AMO activities by the abundance of AOA or AOB genes [8,9,33]. As shown in Figure 2b, the four treatments decreased sharply during days 0–4, and the AMO activities reached a minimum on day 4, with the values of 1.20, 1.23, 1.39, and 1.32 $\text{nmol} \cdot \text{mg}^{-1} \cdot \text{min}^{-1}$, respectively. This decrease may be due to the ammonification of large quantities of $\text{NH}_4\text{-N}$ consuming a large amount of AMO enzyme. After that, the AMO activities gradually increased with the decrease in $\text{NH}_4\text{-N}$ (Figure 1c). The averaged AMO activities during the entire process in the CK, GE, GE + BC, and GE + PL treatments were 1.50, 1.60, 1.70, and 1.67 $\text{nmol} \cdot \text{mg}^{-1} \cdot \text{min}^{-1}$, respectively.

The HAO is the main enzyme for converting hydroxylamine into nitrite nitrogen, and is directly related to the $\text{NO}_3\text{-N}$ of the end product compost [8]. Similar to AMO activities, HAO activities in the four treatments reduced drastically during days 0–4, and then gradually increased until the end of the composting period (Figure 2c). The rapid decrease in HAO activity also corresponded to the rapid increase in $\text{NO}_3\text{-N}$ content (Figure 1d). The average values of the HAO in the CK, GE, GE + BC, and GE + PL treatments' activities during the entire process were 0.41, 0.43, 0.43, and 0.45 $\mu\text{mol K}_3\text{Fe}(\text{CN})_6 \text{h}^{-1}$, respectively. These results showed that GE combined with BC and PL increased the AMO and HAO activities and elevated the process of ammonification, thus improving the subsequent nitrification process and augmenting the final $\text{NO}_3\text{-N}$ content of the compost.

Furthermore, the PCA analysis showed that the three treatments (the GE, GE + BC, and GE + PL treatments) affected the FDA, AMO, and HAO activities relative to the control

treatment (Figure 2d) during the whole composting period. Among the three treatments, samples for the GE + BC treatments on days 4, 13, and 24 were very different to the samples for the GE and GE + PL treatments, which indicated that BC connected GE could effectively change enzymatic activity and has a greater impact on composting process compared to the GE and GE + PL treatments.

3.4. Dynamic Changes in the Abundances of Archaea and Bacteria of the *amoA* Gene

AOA and AOB participate in the oxidation process of ammonia during the composting process [8]. Figure 3 shows the abundance of AOA and AOB genes ranging from 1.12×10^5 – 4.71×10^5 to 3.28×10^4 – 9.13×10^4 copies g^{-1} . During the whole composting process, the gene copies of AOA were higher than those of AOB, which shows that AOA has a greater contribution in accelerated nitrification in this study. This result was in line with the results of Yan et al. [34] on the composting of cattle manure and those of Zeng et al. [8] on the composting of agricultural waste.

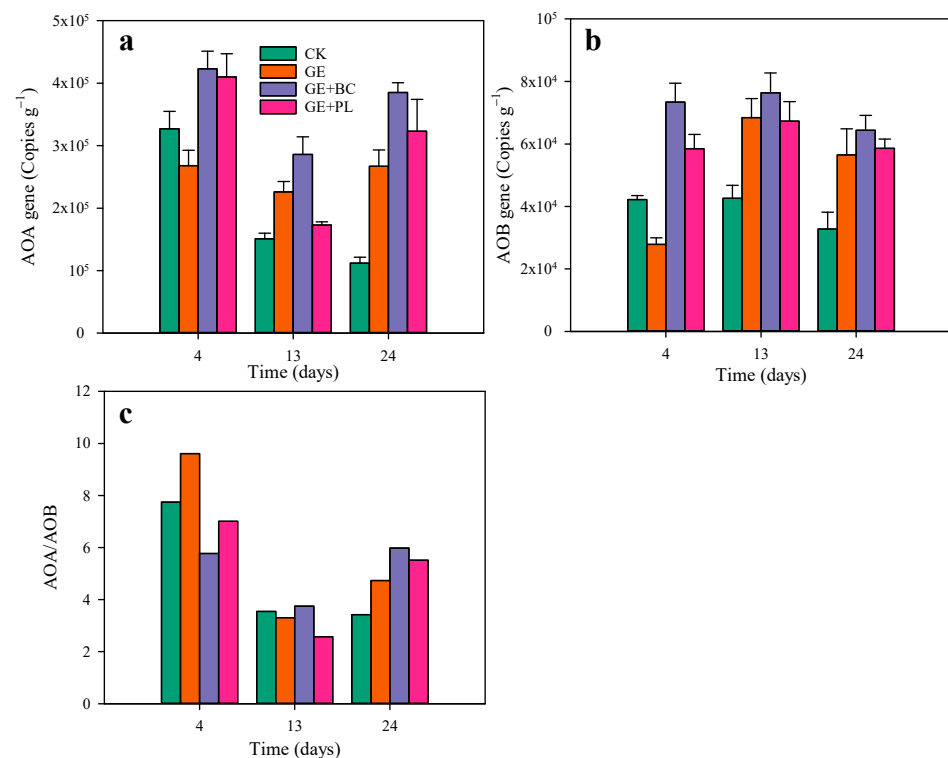


Figure 3. The abundances of AOA (a) and AOB (b) genes and the ratio of AOA to AOB (c).

As shown in Figure 3a, the AOA gene in the CK, GE, GE + BC, and GE + PL treatments during the thermophilic phase (4 d) had the highest values, with values of 3.27×10^5 , 2.68×10^5 , 4.23×10^5 , and 4.10×10^5 copies g^{-1} , respectively. The abundance of the AOA gene in GE was lower than that in the control treatment because of the inhibition of GE by microorganisms. Whereas those in GE + BC and GE + PL were higher than the control mainly due to BC and PL alleviating the inhibition of GE. At the cool stage (13 d), the abundance of the AOA gene decreased, which can be attributed to probable relatively higher temperature during the thermophilic stage slowing down the growth of AOA. After this stage, the temperature dropped and the abundance of the AOA gene simultaneously increased until compost maturity (24 d).

Relative to AOA, the AOB gene had a similar change during the thermophilic phase (Figure 3b). The abundance of AOB genes in the GE + BC and GE + PL treatments on day 4 increased by 73.9% and 38.7%, while in the GE treatment it reduced by 33.8% relative to the control. Wu et al. [10] also reported that BC promoted the abundance of AOB during the composting of agricultural waste. Lin et al. [35] reported that biochar significantly

increased the abundance of the AOA gene, and found that N₂O emissions had an extreme relationship with the abundance of the AOA gene. As the composting process proceeded, the inhibition of GE weakened or was eliminated after the thermophilic phase. This change gradually supported the growth of AOA resulting in an increased abundance of AOA genes during cooling stage. During the cooling and maturity stages, the abundance of the AOA genes in the three additive treatments ranged from 5 to 7 × 10⁵ copies g⁻¹, while this value was 3–4 × 10⁵ copies g⁻¹ in the control.

The ratio of AOA to AOB copies initially decreased during days 4–13, and then increased during days 13–24 (Figure 3c). The results also showed that the AOA copies increased at the cooling and maturity stages relative to AOB, which indicated that AOA could grow well at lower temperatures during the composting process. Sims et al. [5] also reported the better adaptation of AOA than AOB to the low-temperature environment of natural wetlands. Meanwhile, AOB increased during the thermophilic phase, meaning that the high temperature suited the growth of AOB, which also corresponded with the high NH₄-N content (Figure 1c), providing further optimal conditions for AOB [34].

As the results of the AOA and AOB genes shown, the addition of GE slowed down the growth of AOA and AOB, while the addition of BC and PL could eliminate this inhibition during the thermophilic stage. In addition, the gene copies of AOA and AOB in GE + BC and GE + PL were also greater than in the GE and CK treatments during the whole process. This shows that BC and PL combined with GE could improve the growth environment for AOA and AOB, and strengthen nitrification during the composting process, which significantly reduces N₂O emissions (Figure 1b) and increases NO₃-N content (Figure 1d). Meanwhile, other nitrogen functional genes, such as the ammonia monooxygenase (*amoA*), nitrite reductase (*nirK* and *nirS*), and nitrous oxide reductase (*nosZ*) genes, also had close relationships with NH₃ and N₂O emissions [33]. Thus, further research will be necessary to evaluate all nitrogen-functional genes after the addition of additives, which is likely to reveal the mechanism of the nitrogen loss reduction. In addition, this also has important guiding significance for selecting suitable additives to reduce nitrogen loss.

3.5. Community Composition of AOA and AOB

Based on the 16S rDNA sequence data of AOA, a total of 171,053 high-quality sequences were obtained from 12 samples, and clustered into 51 OTUs based on a ≥3% dissimilarity cutoff. Meanwhile, 252,871 sequences and only 14 OTUs were obtained for AOB from the same samples. The results were in line with the relative abundances (Ras) of AOA and AOB genes, and once more affirmed that AOA has a greater contribution to nitrification in this study, relative to AOB.

Principal coordinates analyses (PCoAs), based on unweighted UniFrac distances and the OUT level, were also conducted to explore the difference in species composition among the different treatments. The results showed that the grouping ellipse sizes in GE + BC and GE + PL were bigger than those in the CK and GE treatments, which indicated that BC and PL correlated with GE significantly, which altered the community composition of the AOA (Figure S1).

As shown in Figure 4a, only Crenarchaeota and Thaumarchaeota could be identified as AOA during the composting processes, which is also in line with our previous study when a urease inhibitor and a nitrification inhibitor were added during SS composting [36]. The RAs of these four phyla were 27.55–64.21%, 34.59–63.33%, 0–24.33%, and 0–1.24%, respectively. Significant differences in AOA between treatments (Figure S2) showed that the RA of an unclassified phylum for the GE treatments was lower than for CK, while the RAs for the GE + BC, and GE + PL treatments were greater than the control treatment during thermophilic phase. In the cooling and maturity phases, the RAs of the unclassified phylum in the GE, GE + BC, and GE + PL treatments were all higher than that in the control. The RAs of Crenarchaeota in the GE + BC and GE + PL treatments were lower than in CK during the entire composting process. However, the RA in the GE treatment during thermophilic stage was higher than in the control, while the RA in the GE treatment during

the cooling stage was lower than in the CK treatment. Crenarchaeota widely exist in the ocean, hot springs, and soil, and are the most abundant and most widely distributed AOA in nature [37]. These results not only showed that BC and PL together with GE resulted in the transition from Crenarchaeota to an unclassified phylum, but also indicated the complexity of the community structure of AOA. Thaumarchaeota, as the newly discovered AOA phylum, are highly diverse and widely distributed in various environments, but their physiological metabolism, genetic characteristics, and ecological functions need further study [38]. Thaumarchaeota were only found in the samples of GE + BC₁₃, CK₂₄, and GE₂₄. At the genus level, *unclassified_Archaea*, *norank_Crenarchaeota*, *Nitrososphaera*, and *norank_p_environmental_samples* were the dominant genera of AOA (Figure 4b). These three genera, *unclassified_Archaea*, *norank_Crenarchaeota*, and *norank_p_environmental_samples*, accounted for 75.7–100% of the total sequencing reads. Lin et al. [39] also reported that all of the detected genera belonged to no rank or unclassified genus when treating saline wastewater in biofilm reactors.

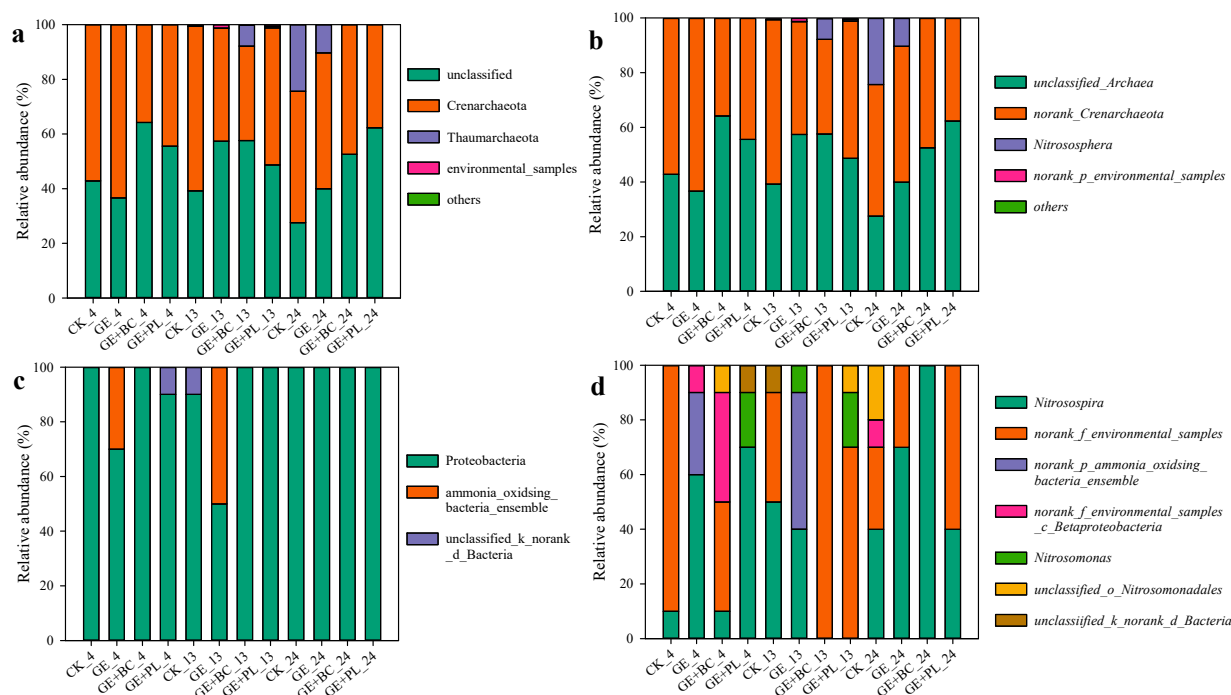


Figure 4. The community composition AOA at the phylum level (a) and at the genus level (b); the community composition AOB at the phylum level (c) and at the genus level (d).

As shown in Figure 4c, only three phyla of AOB, Proteobacteria, ammonia_oxidising_bacteria_ensemble, and unclassified_k_norank_d_Bacteria, were detected in all of the samples during the composting process. The Proteobacteria was the dominant phylum in all samples, while ammonia_oxidising_bacteria_ensemble was only found in the GE₄ and GE₁₃ samples, with the RAs of 30% and 50%, respectively. At the genus level, there were significant differences in the AOB composition between different periods and treatments (Figure 4d). *Nitrosospira* (0–100%), *norank_f_environmental_samples* (0–100%), *norank_p_ammonia_oxidising_bacteria_ensemble* (0–50%), *norank_f_environmental_samples_c_Betaproteobacteria* (0–40%), *Nitrosomonas* (0–20%), *unclassified_o_Nitrosomonadales* (0–20%), and *unclassified_k_norank_d_Bacteria* (0–10%) were the main genera during the composting process. The no-rank and unclassified genera accounted for 75.7–100% of the total sequencing reads. Related to the no-rank and unclassified genera for AOA, these results indicate the complexity of the community structure of AOA and AOB during composting, which urgently requires advanced isolation and identification techniques and the updating of gene databases. Studies have found that *Nitrosospira* and *Nitrosomonas* were the dominant genus for nitrification in many ecosystems, such as sea [30], soil [36], wastewater [39].

On day 4, the RAs of *Nitrosospira* in the GE and GE + PL treatments were significantly greater than in the CK and GE + BC treatments. This can be mainly attributed to the high temperature and $\text{NH}_4\text{-N}$ content in the GE + BC treatment, which ultimately inhibited the *Nitrosospira* genus [40]. Going through the high temperature of the thermophilic stage, the *Nitrosospira* in GE + PL and GE + BC could not be detected on day 13, meaning that the composting conditions were accrual for this specific bacterial genus. With the decrease in temperature during the maturity stages, *Nitrosospira* became the dominant genus with RAs of 40%, 70%, 100%, and 40% in the CK, GE, GE + BC, and GE + PL treatments, and its RAs in the GE + BC treatment reached up to 100%. The high $\text{NO}_3\text{-N}$ content could support this inference. *Nitrosomonas* was the dominant species among the AOB, and Lu et al. [31] found that the RAs of *Nitrosomonas* were up to 79.8% in an anammox-inoculated wastewater treatment system. However, *Nitrosomonas* was only detected in the samples GE + PL_4, GE_13, and GE + PL_13 with RAs of 20%, 10%, and 20%, respectively.

3.6. Relationships between Physicochemical Indexes, Enzymatic Activity, and Ammonia-Oxidizing Microorganisms

The RDA shows that the selected environmental variables (EC, MC, $\text{NH}_4\text{-N}$, $\text{NO}_3\text{-N}$, and C/N) and AMO enzymatic activities could explain 70.8% and 60.1% of the variations in the AOA and AOB community, respectively (Figure 5a,b). Among the seven selected factors, FDA and AMO activities, $\text{NH}_4\text{-N}$, $\text{NO}_3\text{-N}$, and C/N significantly affect the AOA and AOB community structures. FDA represented the overall level of all enzymes and was closely related to the N transformation during the composting process [23]. The AMO enzyme is secreted directly by ammonia-oxidizing microorganisms, consisting of AOA and AOB. Wu et al. [10] also reported that AMO activity had markedly positive relationships with AOA and AOB numbers. As the substrate of ammonia-oxidizing microorganisms, $\text{NH}_4\text{-N}$ content directly affected their structure and abundance. $\text{NO}_3\text{-N}$, as an indirect product of ammonia oxidation, could reflect the evolution of ammonia-oxidizing microorganisms to a certain extent. Shi et al. [6] found that $\text{NO}_3\text{-N}$ solely explained 27.3% of the variation in the AOB species during food waste composting. The initial C/N ratio of composting substrates affects the reproduction of all microorganisms and plays a vital role during the composting process. Lin et al. [35] reported that AOB were positively correlated with $\text{NH}_4\text{-N}$ and C/N, while having an opposite correlation with $\text{NO}_3\text{-N}$.

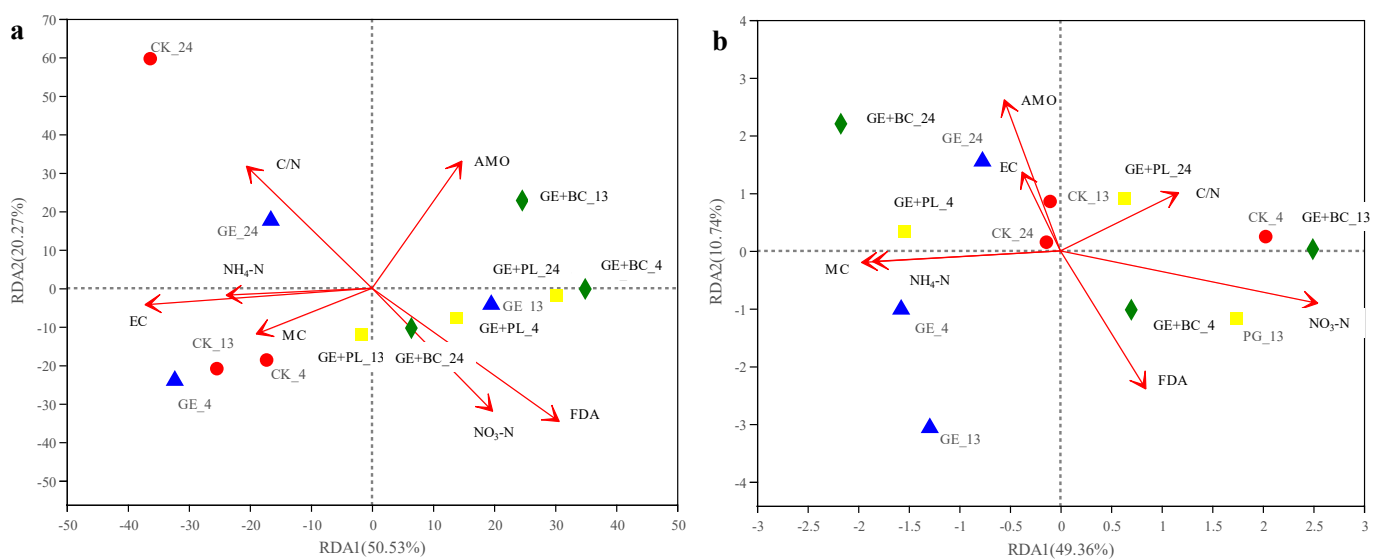


Figure 5. The RDA analysis of enzyme activities, physicochemical indexes, and ammonia-oxidizing microorganisms at the genus level: the RDA of AOA (a) and AOB (b).

In order to analyze the relationships between the three enzymes, eight physicochemical factors, and the detected OTUs (OTU 51 for AOA and OUT 14 for AOB), network analysis

was conducted. The yielded nodes for the AOB community in the CK, GE, GE + BC, and GE + PL treatments were only 13, 4, 3, and 3 (Figure S3), while the corresponding nodes for the AOA community were 20, 25, 26, and 22, respectively (Figure 6). Therefore, only the network analysis related to AOA is presented in the current study.

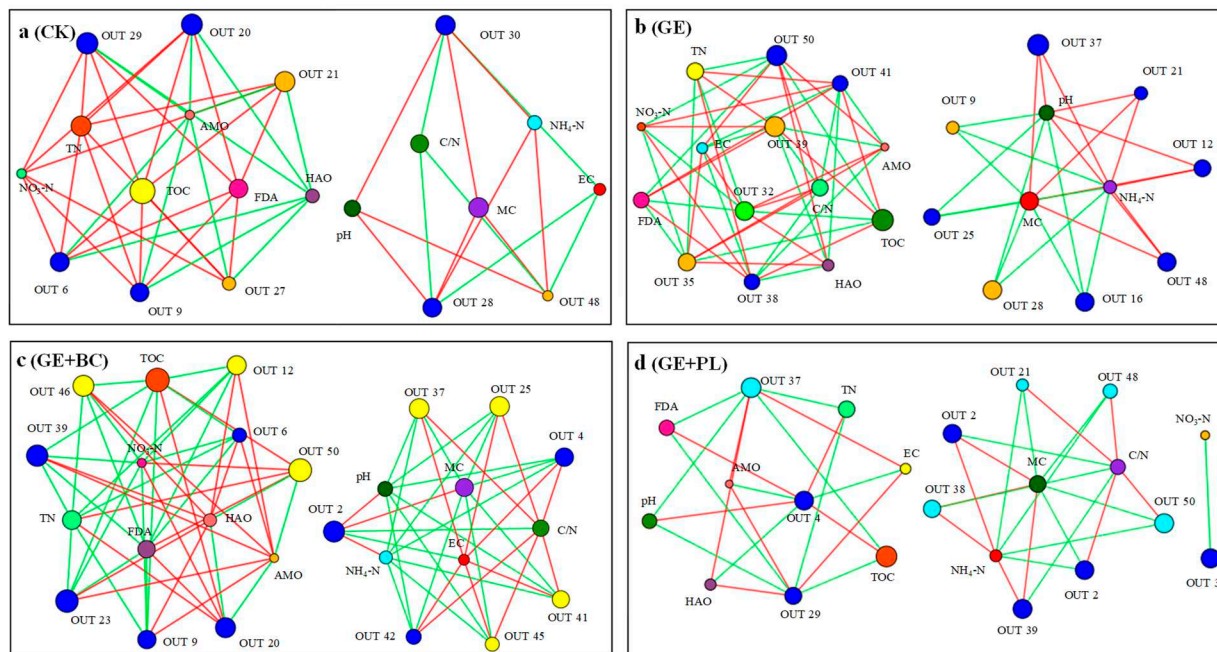


Figure 6. The network analysis of the enzymes, physicochemical characteristics, and the ammonia-oxidizing archaea (AOA) at the OTU level for CK (a), GE (b), GE + BC (c), and GE + PL (d) treatments, respectively. A connection represents a significant correlation ($p < 0.05$) according to Spearman's rank analysis ($\rho > 0.6$).

For the AOA, the analysis revealed 20 nodes and 102 edges, with 11 physicochemical indexes and 9 OTUs in CK. The AMO and HAO activities had negative relationships with OTU 9, OTU 6, OTU 20, OTU 29, OTU 27, and OTU 21 (Figure 6). In the GE treatment, there were 25 nodes and 144 edges, with 11 physicochemical indexes and 14 OTUs. The AMO and HAO activities had positive relationships with OTU 32, OTU 35, and OTU 50, while they negatively correlated with OTU 38, and OTU 41 OTU. For the GE + BC treatment, the analysis revealed 26 nodes and 166 edges, with 11 physicochemical indexes and 15 OTUs. The AMO and HAO activities had positive relationships with OTU 6, OTU 9, OTU 12, OTU 23, OTU 39, and OTU 46, while they had negative relationships with OTU 20 and OUT 50. For the GE + PL treatments, there were 22 nodes and 86 edges, with 11 physicochemical indexes and 11 OTUs. The AMO and HAO activities had positive relationships with OTU 29 and OTU 37, while they had negative relationship with OTU 4.

The OTUs had positive relationships with all AMO and HAO activities belonging to the *unclassified_Archaea* and *norank_Crenarchaeota* genera, indicating that these two genera most probable secreted ammoxidation-related enzymes. Among the three treatments, the close relationships between environmental factors, enzymatic activities, and AOA, were significantly promoted as revealed by the increased numbers of nodes and edges, and the OTUs that had a positive relationship with AMO and HAO activities were also increased in the GE + BC treatment, which showed that the combined usage of GE and BC has the greatest potential to enhance the relationship between enzymes and microorganisms related to ammonia oxidation processes compared to other treatments. Accordingly, this treatment increased the rate of nitrification and reduced NH_3 emissions and N loss during the composting process. Similar results were also reported by Jiang et al. [17] during SS composting.

4. Conclusions

The GE + BC and GE + PL treatments clearly promoted the activities of AMO and HAO and the gene copy numbers of AOA and AOB, thus improving NH₄-N oxidation and NO₃-N production. Meanwhile, the GE + BC and GE + PL treatments decreased NH₃ emissions by 23.8% and 8.3%, respectively. Network analysis showed that the co-application of garbage enzyme with biochar enhanced the positive connections between environmental factors, enzymatic activities, and the dominant genus within AOA. In addition, RDA indicated that FDA and AMO activities, NH₄-N, NO₃-N, and C/N significantly affect the community structures of AOA and AOB. Therefore, GE combined with BC might be a useful strategy to reduce NH₃ emissions and accelerate ammonification during SS composting. Due to the complexity of the community structures of AOA and AOB during composting, further research will be necessary to exploit advanced isolation and identification techniques and the updating of the gene database.

Supplementary Materials: The following supporting information can be downloaded at: <https://www.mdpi.com/article/10.3390/agronomy14061162/s1>, Table S1: The analyze of variance inflation factor; Figure S1: The principal co-ordinates analysis (PCoA) analysis based on unweighted UniFrac distances for the ammonia-oxidizing microorganisms on OUT level: (a) the PCoA nanlysis of AOA, (b) the PCoA nanlysis of AOB; Figure S2: Significant differences in ammonia-oxidizing archaea (AOA) at the phylum level between treatments; Figure S3: The network analysis among the enzymatic activities, physicochemical characteristics, and the ammonia oxidizing bacteria (AOB) at the OTU level. A connection represents a significant correlation ($p < 0.05$) according to Spearman's rank analysis ($\rho > 0.6$).

Author Contributions: Funding acquisition, Supervision, Writing—review & editing, J.J. Writing—original draft, Investigation, H.C. Data curation, Formal analysis, Investigation, P.B. Writing—review & editing, C.C.C.C. Funding acquisition, Supervision, F.Y. Methodology, Resources, Writing—review & editing, Supervision, Validation, D.L. All authors have read and agreed to the published version of the manuscript.

Funding: This research was funded by the National Natural Science Foundation of China (41805123), the Natural Science Foundation of Henan Province (232300421247), and the Yunnan Revitalization Talent Support Program 'Young Talent' Project (YNQR-QNRC-2019-025).

Data Availability Statement: The original contributions presented in the study are included in the article, further inquiries can be directed to the corresponding author.

Acknowledgments: The bacterial community analyses were conducted on the online platform of Majorbio Cloud Platform.

Conflicts of Interest: The authors declare no conflicts of interest.

References

1. Zhao, Y.; Li, W.; Chen, L.; Meng, L.; Zheng, Z. Effect of enriched thermotolerant nitrifying bacteria inoculation on reducing nitrogen loss during sewage sludge composting. *Bioresour. Technol.* **2020**, *311*, 123461. [[CrossRef](#)] [[PubMed](#)]
2. Ruiz-Barrera, O.; Ontiveros-Magadan, M.; Anderson, R.C.; Byrd, A.; Hume, M.E.; Latham, E.A.; Nisbet, D.J.; Arzola-Alvarez, C.; Salinas-Chavira, J.; Castillo-Castillo, Y. Nitro-treatment of composted poultry litter; effects on Salmonella, *E. coli* and nitrogen metabolism. *Bioresour. Technol.* **2020**, *310*, 123459. [[CrossRef](#)] [[PubMed](#)]
3. Lei, L.; Gu, J.; Wang, X.; Song, Z.; Yu, J.; Wang, J.; Dai, X.; Zhao, W. Effects of phosphogypsum and medical stone on nitrogen transformation, nitrogen functional genes, and bacterial community during aerobic composting. *Sci. Total Environ.* **2021**, *753*, 141746. [[CrossRef](#)] [[PubMed](#)]
4. Huang, D.; Gao, L.; Cheng, M.; Yan, M.; Zhang, G.; Chen, S.; Du, L.; Wang, G.; Li, R.; Tao, J.; et al. Carbon and N conservation during composting: A review. *Sci. Total Environ.* **2022**, *840*, 156355. [[CrossRef](#)]
5. Oishi, R.; Tada, C.; Asano, R.; Yamamoto, N.; Suyama, Y.; Nakai, Y. Growth of Ammonia-Oxidizing Archaea and Bacteria in Cattle Manure Compost under Various Temperatures and Ammonia Concentrations. *Microb. Ecol.* **2012**, *64*, 787–793. [[CrossRef](#)]
6. Shi, S.; Zou, D.; Wang, Q.; Xia, X.; Zheng, T.; Wu, C.; Gao, M. Responses of ammonia-oxidizing bacteria community composition to temporal changes in physicochemical parameters during food waste composting. *RSC Adv.* **2016**, *6*, 9541–9548. [[CrossRef](#)]

7. Zhou, S.; Wen, X.; Cao, Z.; Cheng, R.; Qian, Y.; Mi, J.; Wang, Y.; Liao, X.; Ma, B.; Zou, Y.; et al. Modified cornstalk biochar can reduce ammonia emissions from compost by increasing the number of ammonia-oxidizing bacteria and decreasing urease activity. *Bioresour. Technol.* **2021**, *319*, 124120. [[CrossRef](#)] [[PubMed](#)]
8. Zeng, G.; Zhang, J.; Chen, Y.; Yu, Z.; Yu, M.; Li, H.; Liu, Z.; Chen, M.; Lu, L.; Hu, C. Relative contributions of archaea and bacteria to microbial ammonia oxidation differ under different conditions during agricultural waste composting. *Bioresour. Technol.* **2011**, *102*, 9026–9032. [[CrossRef](#)] [[PubMed](#)]
9. Yan, L.; Li, Z.; Wang, G.; Gao, Y.; Wang, Y.; Gu, J.; Wang, W. Diversity of ammonia-oxidizing bacteria and archaea in response to different aeration rates during cattle manure composting. *Ecol. Eng.* **2016**, *93*, 46–54. [[CrossRef](#)]
10. Wu, X.; Ren, L.; Zhang, J.; Peng, H. Effects of zeolite and biochar addition on ammonia-oxidizing bacteria and ammonia-oxidizing archaea communities during agricultural waste composting. *Sustainability* **2020**, *12*, 6336. [[CrossRef](#)]
11. Kuypers, M.M.M.; Marchant, H.K.; Kartal, B. The microbial nitrogen-cycling network. *Nat. Rev. Microbiol.* **2018**, *16*, 263–276. [[CrossRef](#)] [[PubMed](#)]
12. Zhang, L.; Dong, H.; Zhang, J.; Chen, Y.; Zeng, G.; Yuan, Y.; Cao, W.; Fang, W.; Hou, K.; Wang, B.; et al. Influence of FeONPs amendment on nitrogen conservation and microbial community succession during composting of agricultural waste: Relative contributions of ammonia-oxidizing bacteria and archaea to nitrogen conservation. *Bioresour. Technol.* **2019**, *287*, 121463. [[CrossRef](#)] [[PubMed](#)]
13. Arun, C.; Sivashanmugam, P. Identification and optimization of parameters for the semi-continuous production of garbage enzyme from pre-consumer organic waste by green RP-HPLC method. *Waste Manag.* **2015**, *44*, 28–33. [[CrossRef](#)] [[PubMed](#)]
14. Negi, S.; Mandpe, A.; Hussain, A.; Kumar, S. Collegial effect of maggots larvae and garbage enzyme in rapid composting of food waste with wheat straw or biomass waste. *J. Clean. Prod.* **2020**, *258*, 120854. [[CrossRef](#)]
15. Awasthi, M.K.; Duan, Y.; Awasthi, S.K.; Liu, T.; Zhang, Z. Influence of bamboo biochar on mitigating greenhouse gas emissions and nitrogen loss during poultry manure composting. *Bioresour. Technol.* **2020**, *303*, 122952. [[CrossRef](#)] [[PubMed](#)]
16. Ravindran, B.; Nguyen, D.D.; Chaudhary, D.K.; Chang, S.W.; Kim, J.; Lee, S.R.; Shin, J.; Jeon, B.-H.; Chung, S.; Lee, J. Influence of biochar on physico-chemical and microbial community during swine manure composting process. *J. Environ. Manag.* **2019**, *232*, 592–599. [[CrossRef](#)] [[PubMed](#)]
17. Jiang, J.; Wang, Y.; Yu, D.; Zhu, G.; Cao, Z.; Yan, G.; Li, Y. Comparative evaluation of biochar, peletith, and garbage enzyme on nitrogenase and nitrogen-fixing bacteria during the composting of sewage sludge. *Bioresour. Technol.* **2021**, *333*, 125165. [[CrossRef](#)] [[PubMed](#)]
18. Ding, S.; Zhou, D.; Wei, H.; Wu, S.; Xie, B. Alleviating soil degradation caused by watermelon continuous cropping obstacle: Application of urban waste compost. *Chemosphere* **2021**, *262*, 128387. [[CrossRef](#)] [[PubMed](#)]
19. Wang, G.; Li, Y.; Sheng, L.; Xing, Y.; Liu, G.; Yao, G.; Ngo, H.; Li, Q.; Wang, X.C.; Li, Y.; et al. A review on facilitating bio-wastes degradation and energy recovery efficiencies in anaerobic digestion systems with biochar amendment. *Bioresour. Technol.* **2020**, *314*, 123777. [[CrossRef](#)] [[PubMed](#)]
20. Jiang, J.; Pan, Y.; Yang, X.; Liu, J.; Miao, H.; Ren, Y.; Zhang, C.; Yan, G.; Lv, J.; Li, Y. Beneficial influences of peletith and dicyandiamide on gaseous emissions and the fungal community during sewage sludge composting. *Environ. Sci. Pollut. Res.* **2019**, *26*, 8928–8938. [[CrossRef](#)]
21. Jiang, J.; Wang, Y.; Liu, J.; Yang, X.; Ren, Y.; Miao, H.; Pan, Y.; Lv, J.; Yan, G.; Ding, L.; et al. Exploring the mechanisms of organic matter degradation and methane emission during sewage sludge composting with added vesuvianite: Insights into the prediction of microbial metabolic function and enzymatic activity. *Bioresour. Technol.* **2019**, *286*, 121397. [[CrossRef](#)] [[PubMed](#)]
22. Han, Z.; Sun, D.; Wang, H.; Li, R.; Bao, Z.; Qi, F. Effects of ambient temperature and aeration frequency on emissions of ammonia and greenhouse gases from a sewage sludge aerobic composting plant. *Bioresour. Technol.* **2018**, *270*, 457–466. [[CrossRef](#)] [[PubMed](#)]
23. Jiang, J.; Wang, Y.; Yu, D.; Yao, X.; Han, J.; Cheng, R.; Cui, H.; Yan, G.; Zhang, X.; Zhu, G. Garbage enzymes effectively regulated the succession of enzymatic activities and the bacterial community during sewage sludge composting. *Bioresour. Technol.* **2021**, *327*, 124792. [[CrossRef](#)] [[PubMed](#)]
24. Jiang, J.; Kang, K.; Chen, D.; Liu, N. Impacts of delayed addition of N-rich and acidic substrates on nitrogen loss and compost quality during pig manure composting. *Waste Manag.* **2018**, *72*, 161–167. [[CrossRef](#)] [[PubMed](#)]
25. Zhang, M.; He, T.; Chen, M.; Wu, Q. Ammonium and hydroxylamine can be preferentially removed during simultaneous nitrification and denitrification by *Pseudomonas taiwanensis* EN-F2. *Bioresour. Technol.* **2022**, *350*, 126912. [[CrossRef](#)] [[PubMed](#)]
26. Guo, H.; Gu, J.; Wang, X.; Yu, J.; Nasir, M.; Zhang, K.; Sun, W. Microbial driven reduction of N₂O and NH₃ emissions during composting: Effects of bamboo charcoal and bamboo vinegar. *J. Hazard. Mater.* **2020**, *390*, 121292. [[CrossRef](#)] [[PubMed](#)]
27. Liu, C.; Zhang, X.; Zhang, W.; Wang, S.; Fan, Y.; Xie, J.; Liao, W.; Gao, Z. Mitigating gas emissions from poultry litter composting with waste vinegar residue. *Sci. Total Environ.* **2022**, *842*, 156957. [[CrossRef](#)] [[PubMed](#)]
28. Li, X.; Zhao, Y.; Xu, A.; Chang, H.; Lin, G.; Li, R. Conductive biochar promotes oxygen utilization to inhibit greenhouse gas emissions during electric field-assisted aerobic composting. *Sci. Total Environ.* **2022**, *842*, 156929. [[CrossRef](#)] [[PubMed](#)]
29. Geng, X.; Yang, H.; Gao, W.; Yue, J.; Mu, D.; Wei, Z. Greenhouse gas emission characteristics during kitchen waste composting with biochar and zeolite addition. *Bioresour. Technol.* **2024**, *399*, 130575. [[CrossRef](#)] [[PubMed](#)]
30. Li, M.; He, H.; Mi, T.; Zhen, Y. Spatiotemporal dynamics of ammonia-oxidizing archaea and bacteria contributing to nitrification in sediments from Bohai Sea and South Yellow Sea, China. *Sci. Total Environ.* **2022**, *825*, 153972. [[CrossRef](#)] [[PubMed](#)]

31. Lu, J.; Hong, Y.; Wei, Y.; Gu, J.; Wu, J.; Wang, Y.; Ye, F.; Lin, J.-G. Nitrification mainly driven by ammonia-oxidizing bacteria and nitrite-oxidizing bacteria in an anammox-inoculated wastewater treatment system. *AMB Express* **2021**, *11*, 158. [[CrossRef](#)] [[PubMed](#)]
32. Hong, Y.; Wang, Y.; Wu, J.; Jiao, L.; He, X.; Wen, X.; Zhang, H.; Chang, X. Developing a mathematical modeling method for determining the potential rates of microbial ammonia oxidation and nitrite oxidation in environmental samples. *Int. Biodeterior. Biodegrad.* **2018**, *133*, 116–123. [[CrossRef](#)]
33. Liu, B.; Chen, W.; Wang, Z.; Guo, Z.; Li, Y.; Xu, L.; Wu, M.; Yin, H. The Impact of *Bacillus coagulans* X3 on Available Nitrogen Content, Bacterial Community Composition, and Nitrogen Functional Gene Levels When Composting Cattle Manure. *Agronomy* **2024**, *14*, 587. [[CrossRef](#)]
34. Yan, L.; Wang, G.; Ai, S.; Huo, Z.; Wang, Y.; Gu, J.; Wang, W. Abundance of ammonia-oxidizing bacteria and archaea under different ventilation strategies during cattle manure composting. *J. Environ. Manag.* **2018**, *212*, 375–383. [[CrossRef](#)] [[PubMed](#)]
35. Lin, X.; Al-Dhabi, N.A.; Li, F.; Wang, N.; Peng, H.; Chen, A.; Wu, G.; Zhang, J.; Zhang, L.; Huang, H.; et al. Relative contribution of ammonia-oxidizing bacteria and denitrifying fungi to N₂O production during rice straw composting with biochar and biogas residue amendments. *Bioresour. Technol.* **2023**, *390*, 129891. [[CrossRef](#)] [[PubMed](#)]
36. Hu, J.; Richwine, J.D.; Keyser, P.D.; Li, L.; Yao, F.; Jagadamma, S.; DeBruyn, J.M. Ammonia-oxidizing bacterial communities are affected by nitrogen fertilization and grass species in native C4 grassland soils. *PeerJ* **2021**, *9*, e12592. [[CrossRef](#)] [[PubMed](#)]
37. Brochier-Armanet, C.; Boussau, B.; Gribaldo, S.; Forterre, P. Mesophilic crenarchaeota: Proposal for a third archaeal phylum, the Thaumarchaeota. *Nat. Rev. Microbiol.* **2008**, *6*, 245–252. [[CrossRef](#)]
38. Huang, M.; Chai, L.; Jiang, D.; Zhang, M.; Zhao, Y.; Huang, Y. Increasing aridity affects soil archaeal communities by mediating soil niches in semi-arid regions. *Sci. Total Environ.* **2019**, *647*, 699–707. [[CrossRef](#)] [[PubMed](#)]
39. Lin, Z.; Huang, W.; Zhou, J.; He, X.; Wang, J.; Wang, X.; Zhou, J. The variation on nitrogen removal mechanisms and the succession of ammonia oxidizing archaea and ammonia oxidizing bacteria with temperature in biofilm reactors treating saline wastewater. *Bioresour. Technol.* **2020**, *314*, 123760. [[CrossRef](#)] [[PubMed](#)]
40. Zhang, J.; Luo, L.; Gao, J.; Peng, Q.; Huang, H.; Chen, A.; Lu, L.; Yan, B.; Wong, J.W.C. Ammonia-oxidizing bacterial communities and shaping factors with different *Phanerochaete chrysosporium* inoculation regimes during agricultural waste composting. *RSC Adv.* **2016**, *6*, 61473–61481. [[CrossRef](#)]

Disclaimer/Publisher’s Note: The statements, opinions and data contained in all publications are solely those of the individual author(s) and contributor(s) and not of MDPI and/or the editor(s). MDPI and/or the editor(s) disclaim responsibility for any injury to people or property resulting from any ideas, methods, instructions or products referred to in the content.